Acta of Bioengineering and Biomechanics
Vol. 17, No. 3, 2015

Original paper
DOI: 10.5277/ABB-00149-2014-04

Computational simulation analysis for torus radius of edge contact in hip prostheses

FEI LI[1]*, HEJUAN CHEN[1], KEN MAO[2]

[1] School of Mechanical Engineering, Nanjing University of Science and Technology, Nanjing, China.
[2] School of Engineering, University of Warwick, UK.

Stripe wear occurs when the components of hip prostheses move a sufficient distance laterally to contact the edge of the acetabular cup, causing abnormally high contact stresses. In this research, edge loading contact of prosthetic hip is analyzed in the most commonly used material pairs. The contact dimensions and maximal contact pressure are investigated in mutative normal edge loading with 3 different inclination angles (15°, 20°, 25°) and in alterable edge torus radius with edge loading of 2500 N and inclination of 20°. A computational case was conducted for a 14 mm radius alumina ceramic bearing with a radial clearance of 0.1 mm using a normal edge loading ranged from 0 N to 3000 N. Additionally, the Hertzian theory successfully captures principal curvature trends of the edge torus on the influence of maximal contact pressure and obtains the appropriate edge radius range for lower maximal contact pressure. This work elucidates the methods of applying classical contact theory to design the edge radius of hip bearings to better resist severe edge loading contact stresses and reduce the stripe wear.

Key words: *hip prostheses, Hertzian contact, edge torus radius, contact pressure, contact dimensions, inclination angle*

1. Introduction

The acetabular cup and femoral head of a hip prosthesis may not always function as the ideal ball-socket joint that they are designed to be. Hip replacement or resurfacing surgery may change the structural dimensions and the tissue constraints of a hip joint such that the ball and socket are held together more loosely than planned for design. Meanwhile, the increased physical activity and greater life expectancy have caused evident overloading of prosthetic joints [18]. Several studies [21], [9], [17] suggest that the tissue response to wear particles is the main cause of premature failures. Additionally, revision surgery may result in traumatic conditions, high rate of mortality and high cost. Many previous investigations have described various abnormal behaviors in hip prostheses. Dislocation, with the ball head fully departing from the socket, has been widely reported and is the extreme example [11]. A relatively vertical cup orientation may cause edge loading [14], and a recent clinical study found 34% of 1884 acetabular cups to be abducted above the ideal 45° maximum [3]. Dislocation can severely scratch the femoral head [2]. Microseparation can cause ceramic component stripe wear [20], [22]. Thus, when examining the potential wear modes of hip prostheses, it is vital to consider that the joint has the potential to be damaged from adverse behaviors such as disassociation and abnormal contact [1]. In this context, reducing the amount of wear particles is essential for increasing the useful lifespan of the hip prostheses.

In an ideal concentric loading, the ball and socket are in conforming contact, meaning that their contacting surface radii are closely matched; thus, loads produce large contact areas and low contact stresses [1].

* Corresponding author: Fei Li, Nanjing University of Science and Technology, 200 Xiao Ling Wei, Nanjing, 210094, 210094 Nanjing, China. Tel: +86 18260402535, e-mail: 211010001@njust.edu.cn

Received: August 2nd, 2014
Accepted for publication: November 27th, 2014

On the contrary, adverse loading such as edge loading induces high contact stress because the ball and socket come into non-conforming contact, meaning that the contacting surfaces have radii that differ greatly. Under such conditions, loads generate smaller contact areas and higher contact stresses. On the other hand, microseparation inducing stripe wear occurs when the femoral head translates a sufficient distance laterally to contact the edge of the acetabular cup. The change in contact from the conforming spherical surface to non-conforming torus surface of an edge raises the contact stress within the hip prosthesis. Potential solutions to this problem lie in alternative materials and design. Composite ceramic materials with alumina and zirconia have been shown to resist microseparation wear to a greater degree than pure alumina; however, design changes have not been investigated yet [19]. The hypothesis for the study was that the stress could be reduced thereby limiting the degree of fracture and improving bearing longevity by changing the design of the acetabular cup edge's geometric shape.

The Hertzian contact theory has been applied in the case of concentric ceramic-on-ceramic hip contact [13]. In this research, for analyses of adverse loading, the Hertzian theory is also applicable provided that the following assumptions are approximately satisfied: (1) the materials are homogeneous, linear elastic and isotropic and the surfaces are perfectly smooth and frictionless in the case of concentric contact; (2) the surfaces are non-conforming; and (3) the contact dimensions are much smaller than the surface radii at the contact point which is more likely to be valid than in the case of concentric contact [7], [10].

In view of these observations, the aim of this study is to investigate the influence of acetabular cup edge geometry on the resulting contact areas and contact pressure that may occur during microseparation using Hertzian contact theory. This study calculates the contact dimensions and contact pressure of edge-loaded ceramic and metal hip bearings using the Hertzian contact theory.

2. Materials and methods

2.1. Principal curvature of torus surface and Hertzian contact analysis

We can parameterize the torus surface illustrated by Fig. 1 by

$$\begin{cases} x = (R + r\cos v)\cos u, \\ y = (R + r\cos v)\sin u, \\ z = r\sin v, \end{cases} \tag{1}$$

where R and r are the torus' major and minor radii as shown in Fig. 1, respectively, and v is the angle about the torus' minor diameter.

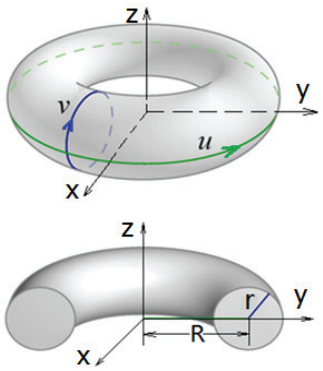

Fig. 1. Torus surface and cross section [8]

Contact between a femoral head and a cup's edge was modeled as a sphere-torus contact as shown in Fig. 2. For a contact point on the torus surface, the

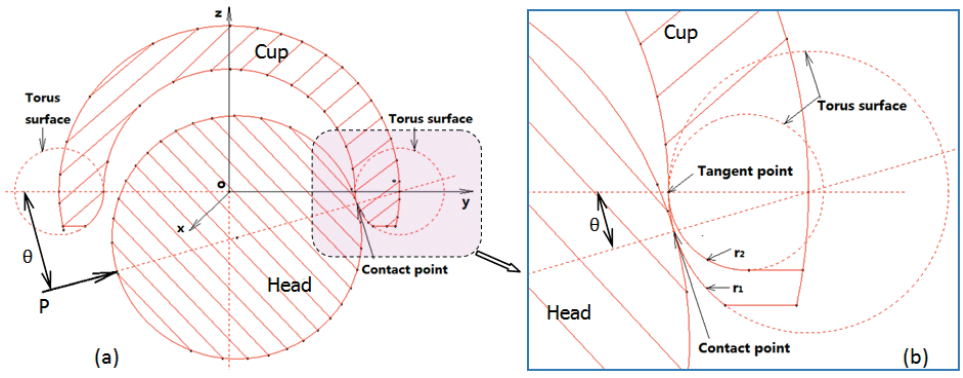

Fig. 2. (a) Model of edge-loaded contact in cross section. An anterior-posterior perspective is given with the entire assembly load vector P vertical and downward; (b) The magnification of contact torus showing in tangent point and contact point

principal curvatures are given by [8]

$$k_{11} = H - \sqrt{H^2 - K}, \quad k_{12} = H + \sqrt{H^2 - K}. \quad (2)$$

Here, K is the Gaussian curvature and H is the mean curvature according to torus parameter equations, which are

$$K = \frac{\cos v}{r(R + r\cos v)}, \quad H = \frac{R + 2r\cos v}{2r(R + r\cos v)}. \quad (3)$$

Equations (3) is substituted into equations (2), then the simplification of equations (2) is as follows

$$k_{11} = \frac{\cos v}{R + r\cos v}, \quad k_{12} = \frac{1}{r}. \quad (4)$$

Given the acetabular cup inclination θ in Fig. 2, v is related to θ as: $v = \pi + \theta$. So, equations (4) can be simplified to

$$k_{11} = \frac{1}{-R \times \sec\theta + r}, \quad k_{12} = \frac{1}{r}. \quad (5)$$

The contact dimensions and maximal contact pressure were computed using Hertzian contact theory. The dimensions of contact ellipse are related to the contacting surfaces as [15]

$$\frac{(1-e^2)^{-1}E(e) - K(e)}{K(e) - E(e)} = \frac{\sum + \Delta}{\sum - \Delta} \quad (6)$$

where

$$\begin{cases} \sum = k_{11} + k_{12} + k_{21} + k_{22}, \\ \Delta = [(k_{11} - k_{12})^2 + (k_{21} - k_{22})^2 \\ \quad + 2(k_{11} - k_{12})(k_{21} - k_{22})\cos(2\beta)]^{1/2}, \\ e = \sqrt{1 - b^2/a^2}, \end{cases} \quad (7)$$

here, $k_{21} = k_{22}$ is the principal curvature of the sphere, and $\beta = 0$ because one contact surface is spherical. e is named elliptic eccentricity. a and b are the contact ellipse's major semi-axis and minor semi-axis, respectively. $K(e)$, $E(e)$ are the 1st and 2nd complete elliptic integrals of relating to the argument e, respectively: $K(e) \equiv \int_0^{\pi/2} 1/\sqrt{1 - e^2\sin^2\varphi}\, d\varphi$, $E(e) \equiv \int_0^{\pi/2} \sqrt{1 - e^2\sin^2\varphi}\, d\varphi$. And because equation (6) is a transcendental equation which is made up of higher transcendental integral functions, e is only calculated numerically from it.

From Hertz's integral formulas [13], two formulas for the contact ellipse dimensions are derived

$$a = \left\{ \frac{6P[K(e) - E(e)]}{\pi e^2 E^* (\sum - \Delta)} \right\}^{1/3}, \quad b = \left\{ \frac{6P\sqrt{1-e^2}[E(e) - (1-e^2)K(e)]}{\pi e^2 E^* (\sum + \Delta)} \right\}^{1/3} \quad (8)$$

where the contact bodies' Young's moduli E_1, E_2 and Poisson's ratios v_1, v_2 exist within equivalent modulus $E^* = [(1 - v_1^2)/E_1 + (1 - v_2^2)/E_2]^{-1}$. The maximum contact pressure is $p_0 = 3P/(2\pi ab)$ [10].

2.2. Contact computation

The computation created static contact between the femoral head and specified contact points of cup edge as shown in Fig. 2. The relevant material properties and physical conditions needed in the computation are given in Table 1.

Table 1. Physical conditions of Hertz contact

Name	Symbol	Value
Formal head radius	R_h	14 mm
Cup inner radius	R_c	14.1 mm
Young's modulus of head (CoCr)	E_h	230 GPa
Young's modulus of cup (alumina)	E_c	300 GPa
Poisson's ratio of head	v_h	0.3
Poisson's ratio of cup	v_c	0.26
Normal load	P	0~3000 N
Inclination angle	θ	15°, 20°, 25°
Torus radius	r	0~80000 mm
Torus axis radius	$R = r + R_c$	

3. Results

Contact parameters for the cup edge designs as functions of edge loading and edge radius are shown graphically in Fig. 3 and Fig. 4. Figure 3 shows the contact patch dimensions and maximal contact pressure with mutative load vector P in different cup inclination angles (15°, 20°, 25°) from each edge radius. The dimensional results and maximal contact pressure with different edge radius are given in Fig. 4 when the load P is 2500 N and the cup inclination angle is 20°. Table 2 summarizes the results considering the entire edge radius ranges with three different inclination angles. Under the same conditions, the contact dimensions and maximal contact pressure should increase in

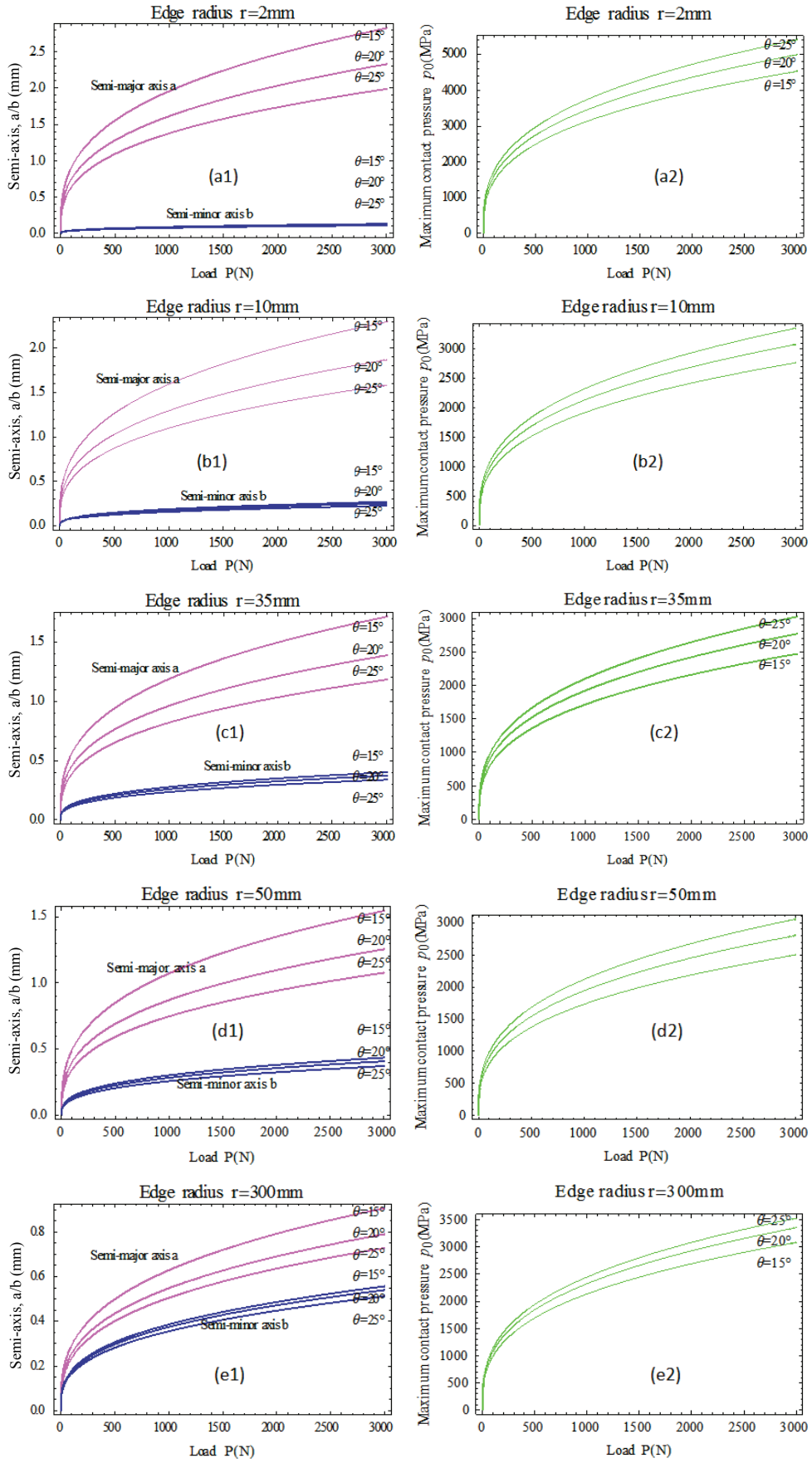

Fig. 3. (a1–e1) the contact dimensions *a* and *b* with mutative load vector *P* in different cup inclination angles; (a2–e2) Maximal contact pressure of different radiuses

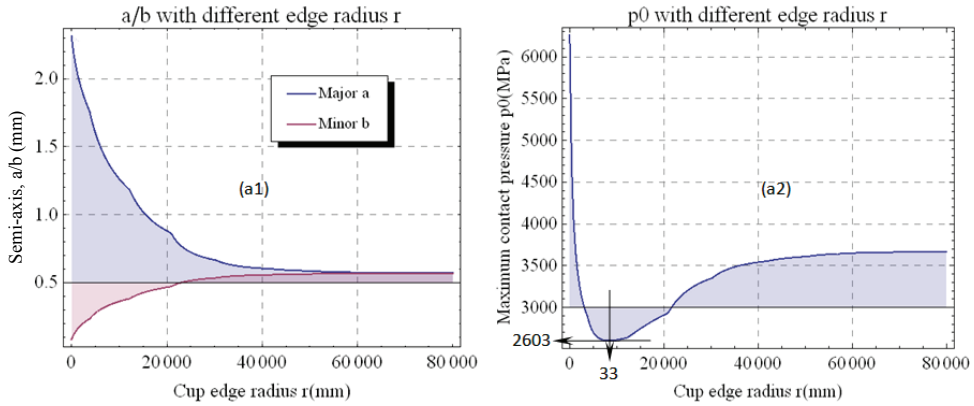

Fig. 4. The schematic diagram of contact dimensions and maximal contact pressure along with cup edge radius

Table 2. Computational contact dimensions and maximal contact pressure, summarized over some edge radiuses with the load P = 2500 N

r [mm]	θ [°]	a [mm]	b [mm]	p_0 [MPa]
2	15	2.65726	0.105263	4267.46
	20	2.19016	0.115854	4704.28
	25	1.86980	0.125272	5096.05
10	15	2.16355	0.212097	2601.24
	20	1.76012	0.234374	2893.54
	25	1.49259	0.253534	3154.30
35	15	1.62719	0.315743	2323.32
	20	1.31722	0.347978	2604.19
	25	1.12244	0.373650	2846.11
50	15	1.45477	0.348796	2352.42
	20	1.18144	0.382927	2638.49
	25	1.01364	0.409076	2878.67
300	15	0.852939	0.482459	2900.70
	20	0.743637	0.508526	3156.36
	25	0.685480	0.524027	3323.02

accuracy with increasing edge load vector P, and vice versa in Fig. 3. The contact dimensions will decrease while maximal contact pressure increases when increasing the cup inclination angle at a certain edge load. All edge radius designs showed decreasing contact semi-major axis and increasing contact semi-minor axis with increasing edge radius. However the maximal contact pressure should decrease initially and then increase with augmenting edge radius. Thereby the radius design produced the least maximal contact pressure (2603 MPa) at an edge radius of 33 mm.

4. Discussion

4.1. Contact dimensions and maximal pressure with mutative edge loading

A study has provided extensive evidence that the accuracy of the Hertzian contact theory for predicting contact dimensions and contact pressure in edge loading depends on the bearing materials and the contact position [1].

That finding is valuable because it implies that the Hertzian theory may be used to predict edge loading contact stresses [5]. Little is currently known about the in-vivo contact loads experienced during subluxation; therefore, this study examined widely varying loads and edge radiuses to reflect the likelihood that in-vivo contact loads and radius span a broad range, expecting reducing adverse wear.

It was reported that alumina maintains an elastic Hertzian response up to a mean contact pressure of 5 GPa (maximal pressure is 7.5 GPa) [6]. In the present computation of the Φ28 mm pair, the maximum predicted mean pressure was 4.2 GPa, with p_0 = 6.3 GPa (θ = 20°, r = 1 mm, P = 2500 N) as shown in Fig. 4 (a2); thus, based on the prior research, all the present contact pairs were within the elastic range. In spite of predicted plasticity, the contact patches were elliptical, and both a and b followed the trends predicted by the Hertzian theory as shown in Fig. 3. The contact dimensions increase with increasing edge load P in each given edge radius r including three cup inclination angles as shown in Fig. 3 from (a1) to (e1) vertically. In contrast, the maximal contact pressure was not this case. It seems that maximal contact pressure reduces initially and then ascends with increasing edge radius, showing in Fig. 4 from (a2) to (e2) vertically at the previous conditions. Thus, to recognize the pressure's variational law, it is still further required to compute the maximal contact pressure when the edge radius increases so as to proclaim the variational tendency clearly. As described below, our results exhibited trends consistent with the prediction in Fig. 3 as shown in Fig. 4.

4.2. The appropriate edge radius with the lowest maximal contact pressure

As known, the contact pressure caused by edge loading is much greater than that caused by concentric contact. For example, with the Φ36 mm Al_2O_3 pair edge loaded to 1000 N (θ = 16.1°, r = 4 mm), P_{max} is 1950 MPa, but for concentric contact, it is only 45 MPa [1]. Similar dramatic differences were reported in an FEA of microseparation [13]. Researchers reported contact pressures of 4100 MPa for headliner contact in FEA of edge-loaded hard bearings [4]. In Fig. 4 (a1), the contact dimensions (semi-axis *a* and *b*) have the same trends as illustrated in Fig. 3 that is the decreasing and increasing of semi-axis *a* and *b* respectively with the ascending edge radius at a fixed load of 2500 N. However, in Fig. 4 (a2) the maximal contact pressure was not the case. It seems that maximal contact pressure reduces rapidly at first and then ascends slowly with increasing edge radius continuously. Interestingly, the 33 mm edge radius design reduced the maximum contact pressure to 2603 MPa that was just verified the lowest point of that section above comparing with other edge radiuses. The cup edge with a radius of 33 mm is very effective in reducing the contact stress. As the predicted maximum contact pressure dropped considerably and to a magnitude below the maximal strength 7.5 GPa of the alumina mentioned above, this would support a lower steady-state wear rate as observed in *in vitro* studies [23]. Additionally, the appropriate edge radius is 33 mm with the minimal maximum contact pressure for the Φ36 mm CoC pair in this research, helping to reduce scratching stripe wear.

The present study's computational results and analytical methods may serve to experimentally validate such analyses. The authors would like to raise concern that introducing an appropriate edge radius, while reducing the stress, may affect the biomechanics during microseparation and result in a greater degree of translation [12]. Future studies will address dynamic analysis of contact pair impacts and further tangent point of torus surface studies investigating edge radius position designs with different cup inclination angles.

5. Conclusions

Elucidating Hertzian contact computational method of edge contacts is always difficult due to the complicated nature of the contact. The results of this study suggest that edge loading of alumina hips increases the maximum contact pressure in the acetabular cup to a level where it may exceed the flexural strength of the ceramic material. Once the appropriate edge radius with the lowest maximum contact pressure had been chosen for a certain pair in this research, the acetabular cup was predicted to reduce the maximal contact pressure dramatically. The results help to improve the design of edge radius in vitro studies.

Acknowledgments

We gratefully acknowledge Elsevier, Professional Engineering Publishing and IOP Publishing for permission to reprint some contents taken from their publications. Also the authors would like to express their gratitude to Smith & Nephew Orthopedics Co. Ltd., for their support and suggestions with the understanding of artificial hip joint products.

References

[1] ALI M., MAO K., *Contact analysis of hip resurfacing devices under normal and edge loading conditions*, IAENG Special Issues Journal, 2012, Vol. 20(4), 317–329.

[2] BOURNE R.B., BARRACK R., RORABECK C.H., SALEHI A., GOOD V., *Arthroplasty options for the young patient: oxinium on cross-linked polyethylene*, Clin. Orthop. Relat. R, 2005, Vol. 441, 159–167.

[3] CALLANAN M.C., JARRETT B., BRAGDON C.R., ZURAKOWSKI D., RUBASH H.E., FREIBERG A.A., MALCHAU H., *The John Charnley Award: risk factors for cup malpositioning: quality improvement through a joint registry at a tertiary hospital*, Clin. Orthop. Relat. R, 2010, Vol. 18, 18–28.

[4] ELKINS J.M., O'BRIEN M.K., STROUD N.J., PEDERSEN D.R., CALLAGHAN J.J., BROWN T.D., *Hard-on-hard total hip impingement causes extreme contact stress concentrations*, Clin. Orthop. Relat. R, 2011, Vol. 469, 454–463.

[5] FABRIKANT V.I., *A new symbolism for solving the Hertz contact problem*, Q. J. Mech. Appl. Math., 2005, Vol. 58, 367–381.

[6] GUIBERTEAU F., PADTURE N.P., LAWN B.R., *Effect of grain size on hertzian contact damage in alumina*, J. Am. Ceram. Soc., 1994, Vol. 77, 1825–1831.

[7] HERTZ H., *On The contact of rigid elastic solids and on hardness*, [in:] J.A. Schott (ed.), Miscellaneous Papers by H. Hertz, Macmillan, London, 1882, 164–183.

[8] IRONS M.L., *The curvature and geodesics of the torus*. http://www.rdrop.com/half/math/torus/index.

[9] JACOBS J.J., ROEBUCK K.A., ARCHIBECK M., HALLAB N.J., GLANT T.T., *Osteolysis: basic science*, Clin. Orthop. Relat. R., 2001, Vol. 393, 71–77.

[10] JOHNSON K.L., *Contact Mechanics*, Cambridge University Press, 1985.

[11] LEWINNEK G.E., LEWIS J.L., TARR R., COMPERE C.L., ZIMMERMAN J.R., *Dislocations after total hip-replacement arthroplasties*, J. Bone Joint Surg. Am., 1978, Vol. 60, 217–220.

[12] MAK M., JIN Z., FISHER J., STEWART T.D., *Influence of acetabular cup rim design on the contact stress during edge*

loading in ceramic-on-ceramic hip prostheses, J. Arthroplasty, 2011, Vol. 26, 131–136.

[13] MAK M.M., JIN Z.M., *Analysis of contact mechanics in ceramic-on-ceramic hip joint replacements, proceedings of the institution of mechanical engineers*, Part H: J. Eng. Med., 2002, Vol. 216, 231–236.

[14] MELLON S.J., SIMPSON D.J., KWON Y.M., MURRAY D.W., GILL H.S., *The influence of acetabular component orientation on stress during gait in metal-on-metal hip resurfacing*, in: Proceedings Of The 56th Annual Meeting Of The Orthopaedic Research Society, New Orleans, 2010.

[15] NIKAS G.K., *Fatigue life and traction modeling of continuously variable transmissions*, J. Tribol-T Asme, 2002, Vol. 124, 689–698.

[16] SANDERS A.P., BRANNON R.M., *Assessment of the applicability of the Hertzian contact theory to edge-loaded prosthetic hip bearings*, J. Biomech., 2011, Vol. 44, 2802–2808.

[17] SCHMALZRIED T.P., JASTY M., HARRIS W.H., *Periprosthetic bone loss in total hip arthroplasty polyethylene wear debris and the concept of the effective joint space*, J. Bone Joint Surg. Am., 1992, Vol. 74(6), 849–863.

[18] SILVA M., SHEPHERD E.F., JACKSON W.O., DOREY F.J., SCHMALZRIED T.P., *Average patient walking activity approaches 2 million cycles per year: pedometers under-record walking activity*, J. Arthroplasty, 2002, Vol. 6(17), 693–697.

[19] STEWART T.D., TIPPER J.L., INSLEY G., STREICHER R.M., INGHAM E., FISHER J., *Long-term wear of ceramic matrix composite materials for hip prostheses under severe swing phase microseparation*, J. Biomed. Mater Res., 2003, Vol. 66B, 567–573.

[20] WALTER W.L., INSLEY G.M., WALTER W.K., TUKE M.A., *Edge loading in third generation alumina ceramic-on-ceramic bearings: Stripe Wear*, J. Arthroplasty, 2004, Vol. 19, 402–413.

[21] WILLERT H.G., BERTRAM H., BUCHHORN G.H., *Osteolysis in Alloarthroplasty of the hip, the role of ultra-high molecular weight polyethylene wears particles*, Clin. Orthop. Relat. R, 1990, Vol. 258, 95–107.

[22] YAMAMOTO T., SAITO M., UENO M., HANANOUCHI T., TOKUGAWA Y., YONENOBU K., *Wear analysis of retrieved ceramic-on-ceramic articulations in total hip arthroplasty: femoral head makes contact with the rim of the socket outside of the bearing surface*, J. Biomed. Mater Res. B, Applied Biomaterials, 2005, Vol. 73, 301–307.

[23] ZENG P., INKSON B.J., RAINFORTH W.M., STEWART T., *3D surface reconstruction and FIB microscopy of worn alumina hip prostheses*, J. Phys., 2008, Conference Series 126, Art. No. 012044.